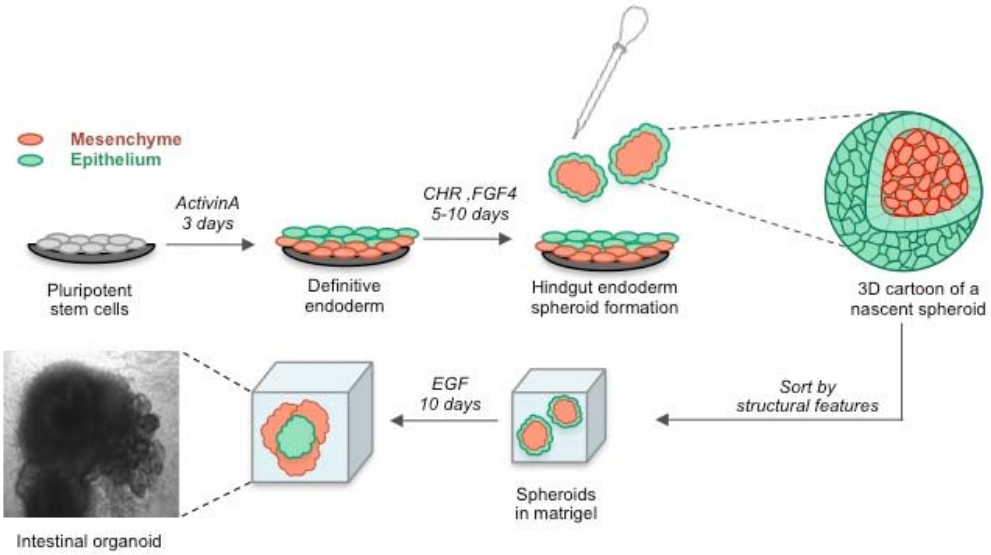

Figure S1: Schematic of directed differentiation. hPSCs were differentiated to a hindgut fate through a definitive endoderm intermediate. Spheroids that budded off of the hindgut cultures were sorted and cultured under organoid growth conditions.

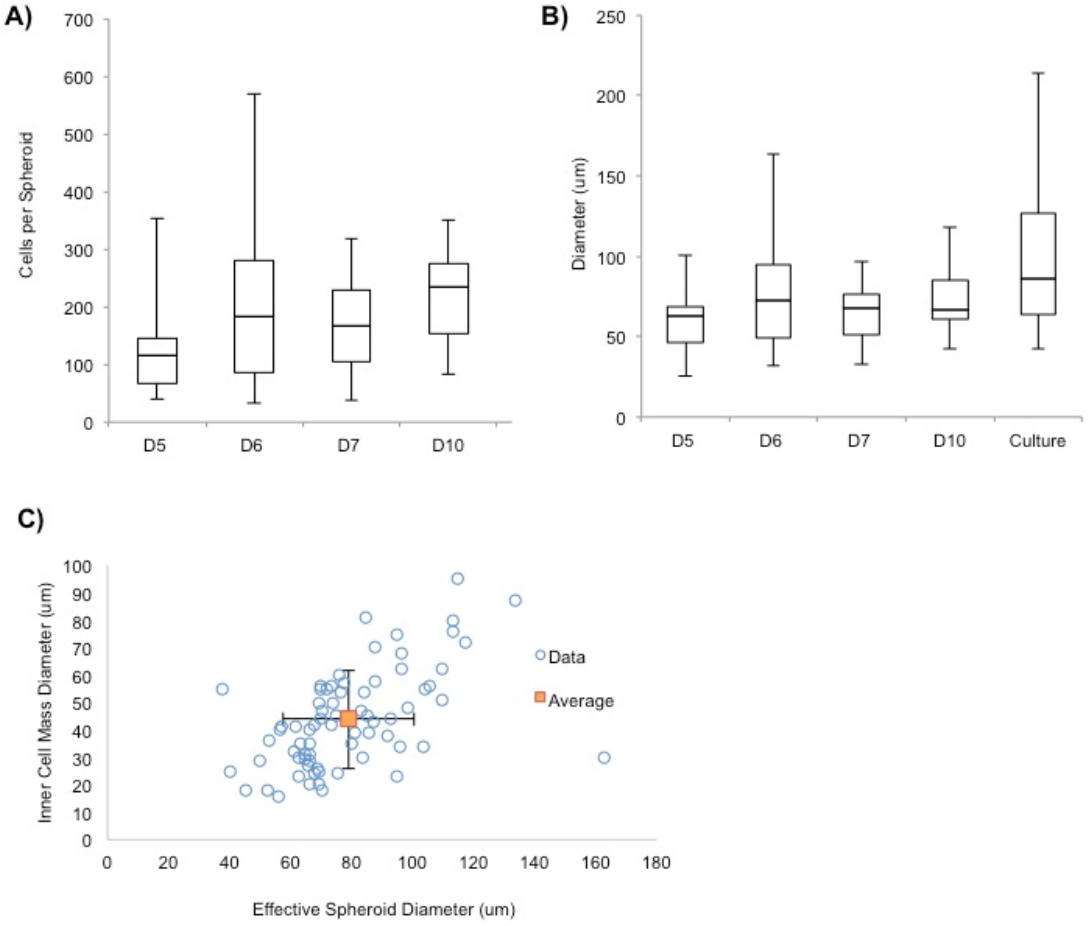

Figure S2: Quantification of spheroid size. Box-and-whisker plots showing the distribution of the **A)** number of cells per spheroid and **B)** spheroid diameters (defined as the average of the major and minor axes) of spheroids from days 5, 6, 7, and 10 of hindgut induction. **C)** Scatter plots showing correlations between spheroid diameter (μm) and the diameter of the inner cell mass (μm). Standard deviation is indicated.

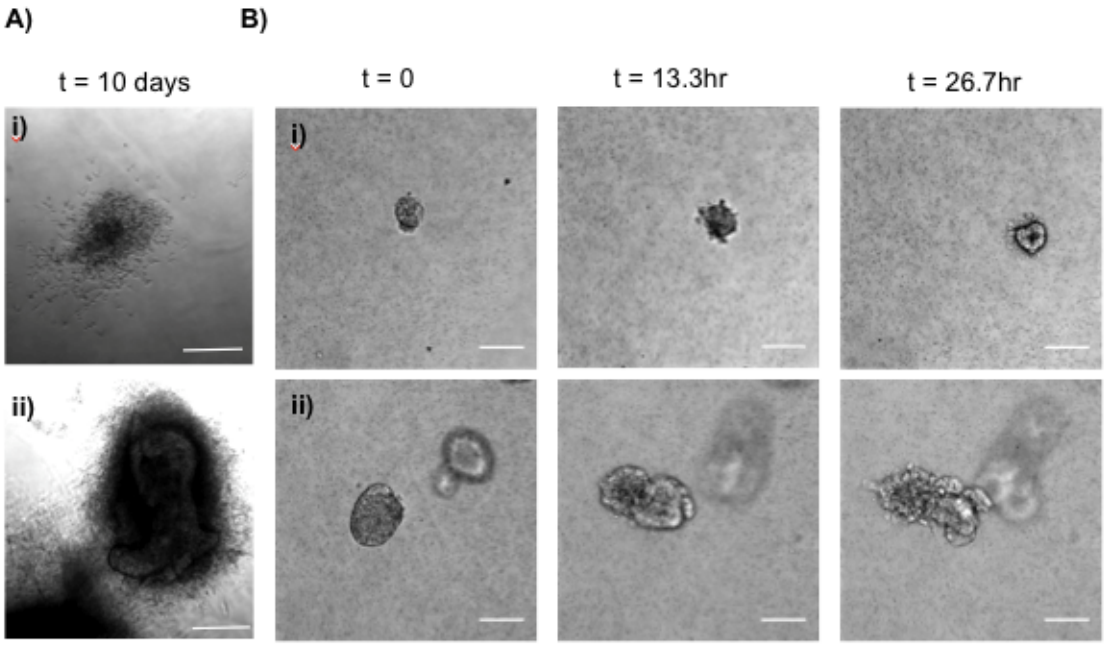

Figure S3: Spheroid growth. **A)** Brightfield image after 10 days in matrigel of **i)** a spheroid that did not mature and **ii)** a spheroid that did mature. **B)** Brightfield images of spheroids at time 0, 13.3 hours, and 26.7 hours after embedding in matrigel. The spheroid in **i)** will likely stagnate, while the spheroid in **ii)** will like mature. Scale bar = 100 μm.

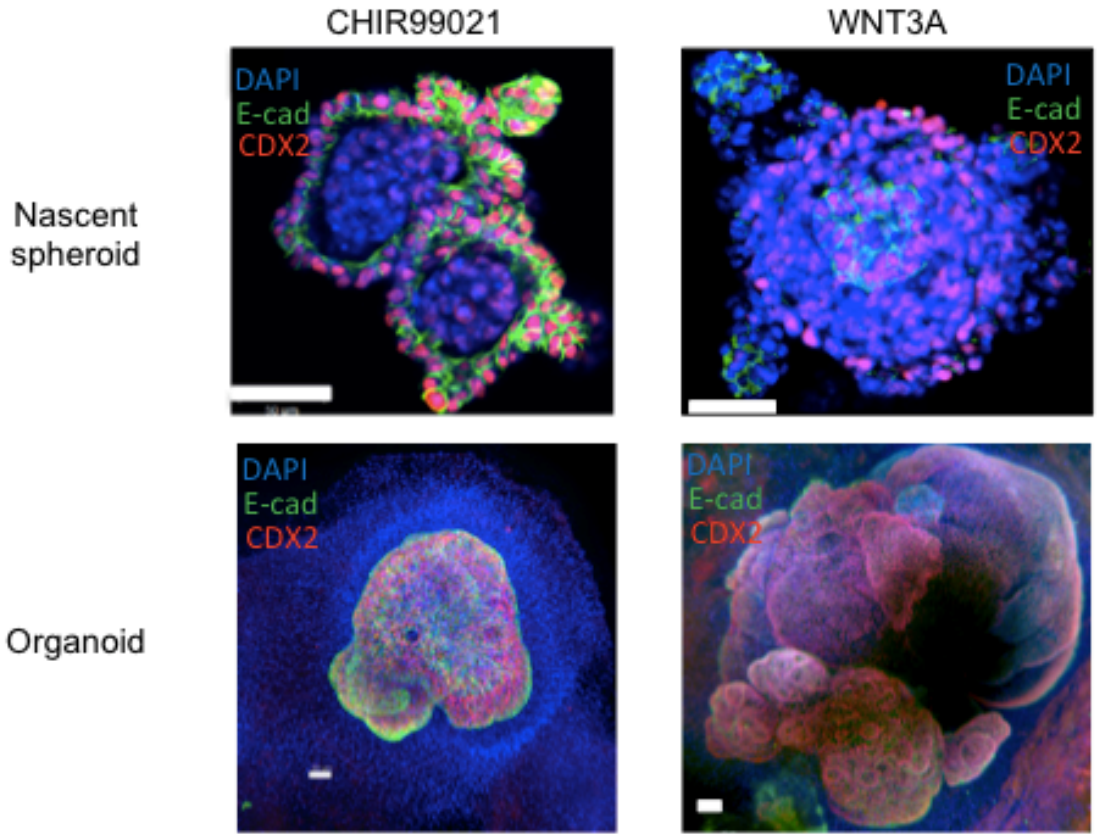

Figure S4: Spheroids with reversed organization. Representative images of spheroids with an inner mass that emerged from cultures treated with CHIR99021 or WNT3A and wholemount immunofluorescence microscopy images of the resulting organoids. Epithelial marker E-cadherin is in green, hindgut marker CDX2 is in red, and nuclear stain DAPI is in blue. Scale bar = 50 μm.

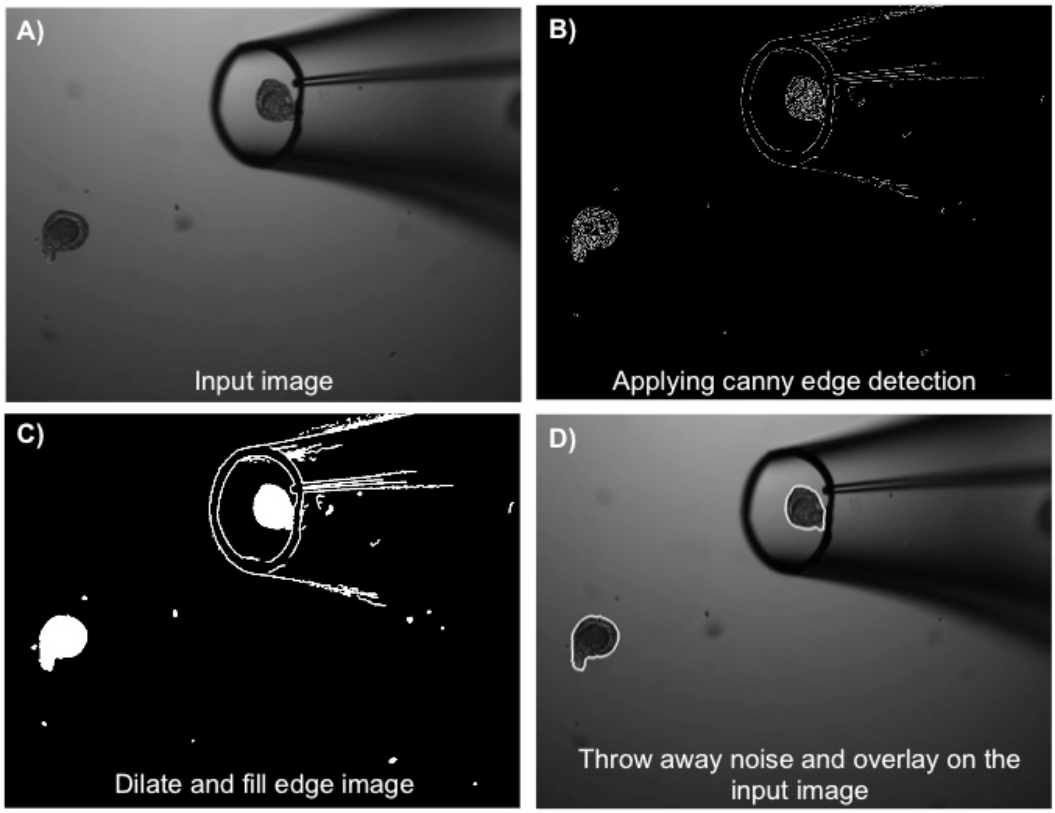

Figure S5: 2D brightfield spheroid image segmentation. **A)** Input image. **B)** Image after canny edge detection. **C)** Filling holes between edges. **D)** De-noising and overlaying found spheroids on original image.

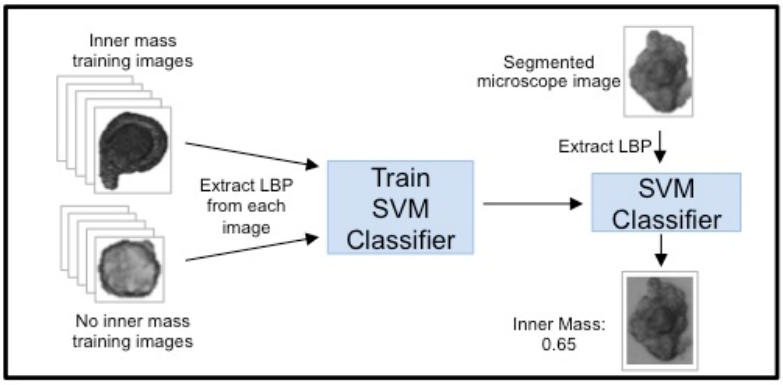

Figure S6: Spheroids classified by morphology. Local binary patterns (LBP) feature vectors were extracted from two sets of images, one labeled as having an inner mass and one labeled as not having an inner mass. These feature vector-label pairs were used to train a support vector machine (SVM) classifier. Finally, segmented microscope images were classified by the SVM and displayed along with a confidence score. The user verified the classification before proceeding.

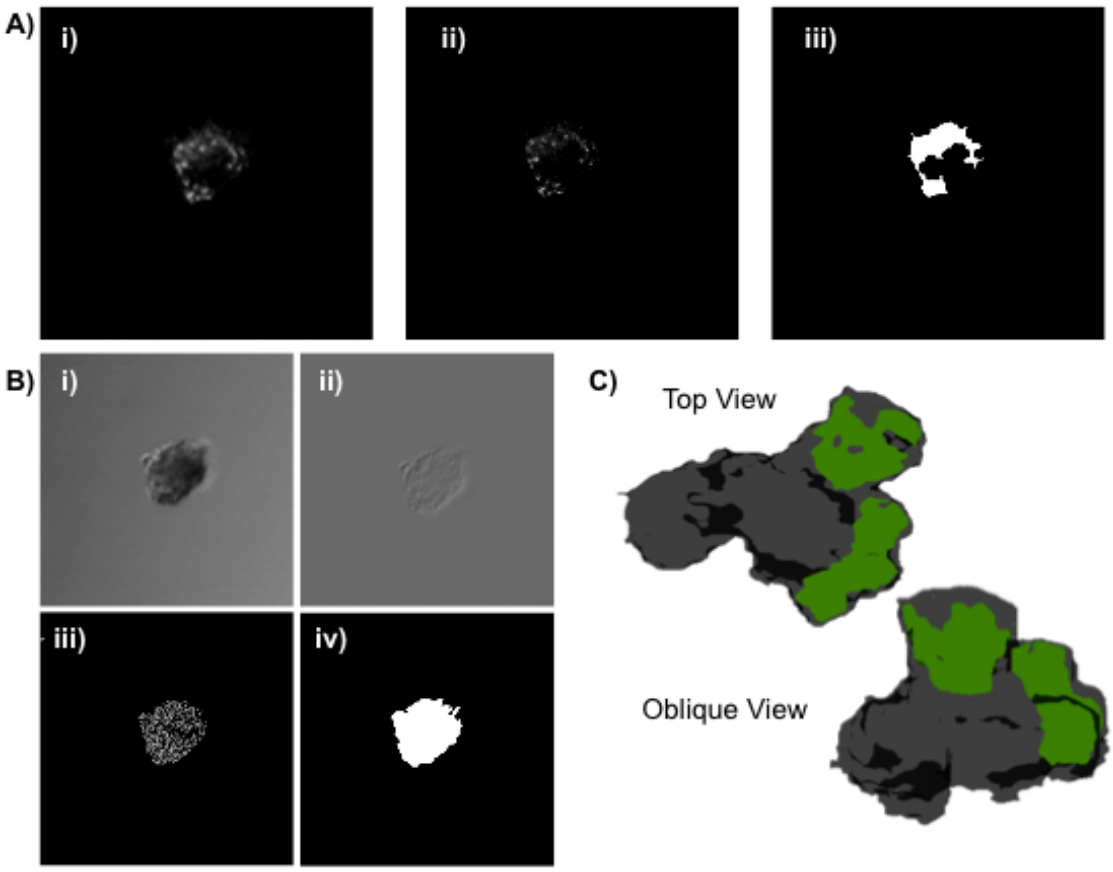

Figure S7: 3D spheroid image brightfield and Alexa Fluor 488 segmentation and reconstruction. **A)** Segmentation of single slice of the Alexa Fluor 488 image stack, **i)** from the original image, **ii)** denoising the image, **iii)** to the final segmented image after thresholding. **B)** Segmentation of single slice of the brightfield image stack, **i)** from the original image, **ii)** taking the magnitude of the spatial gradient, **iii)** applying Canny edge detection, **iv)** to the final segmentation result. **C)** Representative reconstruction of a different spheroid from the segmented Alexa Fluor 488 and brightfield image stacks. E-cadherin positive areas are shown in green while grey areas show the total volume of the spheroid. This spheroid has two distinct Alexa Fluor 488 regions.

Table S1: Not harvested and harvested spheroid maturation.

Observed /Type	Not harvested	Harvested
Matured	314	219
Did not mature	2402	1550
Percent matured	12%	12%

Table S2: Spheroid maturation after live E-cadherin staining.

Observed /Type	No antibody	Antibody
Matured	339	378
Did not mature	845	987
Percent matured	29%	28%